MODELLING CLIMATE CHANGE EFFECTS ON ATLANTIC SALMON: IMPLICATIONS FOR MITIGATION IN REGULATED RIVERS

RUNING HEAD: MITIGATING CLIMATE CHANGE EFFECTS IN ATLANTIC SALMON

Sundt-Hansen, L. E. [a*], R. D. Hedger [a], O. Ugedal [a], O. H. Diserud [a], A Finstad [a, 5], J. F. Sauterleute[b,4], L.Tøfte[2], K. Alfredsen[c] & T. Forseth [a]

[a] *Norwegian Institute for Nature Research, P.O. Box 5685 Sluppen 7485, Trondheim, Norway,*

[b] *SINTEF Energy Research, P.O. Box 4761 Sluppen 7465 Trondheim, Norway,*

[c] *Norwegian Department of Hydraulic and Environmental Engineering, Norwegian University of Science and Technology,7491 Trondheim, Norway.*

[d] *SWECO, Professor Brochs gate 2, 7030, Trondheim, Norge.*

[e] *Department of Natural History, Norwegian University of Science and Technology, 7491 Trondheim.*

[*]Corresponding author: Line Elisabeth Sundt-Hansen, phone: +47 98421195, e-mail: line.sundt-hansen@nina.no

Key-words: salmonids, individual-based modelling, population abundance, hydropower regulation, mitigation, climate scenarios

This is the accepted version of an article published in Science of the Total Environment
DOI: 10.1016/j.scitotenv.2018.03.058

ABSTRACT

Climate change is expected to alter future temperature and discharge regimes of rivers. These regimes have a strong influence on the life history of most aquatic river species, and are key variables controlling the growth and survival of Atlantic salmon. This study explores how the future abundance of Atlantic salmon may be influenced by climate-induced changes in water temperature and discharge in a regulated river, and investigates how negative impacts in the future can be mitigated by applying different regulated discharge regimes during critical periods for salmon survival. A spatially explicit individual-based model was used to predict juvenile Atlantic salmon population abundance in a regulated river under a range of future water temperature and discharge scenarios (derived from climate data predicted by the Hadley Centre's Global Climate Model (GCM) HadAm3H and the Max Plank Institute's GCM ECHAM4), which were then compared with populations predicted under control scenarios representing past conditions. Parr abundance decreased in all future scenarios compared to the control scenarios due to reduced wetted areas (with the effect depending on climate scenario, GCM, and GCM spatial domain). To examine the potential for mitigation of climate change-induced reductions in wetted area, simulations were run with specific minimum discharge regimes. An increase in abundance of both parr and smolt occurred with an increase in the limit of minimum permitted discharge for three of the four GCM/GCM spatial domains examined. This study shows that, in regulated rivers with upstream storage capacity, negative effects of climate change on Atlantic salmon populations can potentially be mitigated by release of water from reservoirs during critical periods for juvenile salmon.

1. INTRODUCTION

Climate change is expected to modify thermal and hydrological regimes of rivers, with uncertain consequences for aquatic species (Knouft & Ficklin, 2017). In the Northern

This is the accepted version of an article published in Science of the Total Environment
DOI: 10.1016/j.scitotenv.2018.03.058

Hemisphere, climate models have predicted an increase in air temperature and winter precipitation, but a decrease in summer precipitation (IPCC, 2007; Schneider *et al.*, 2013). For Southern Norway, run-off is expected to increase in winter, but decrease in summer (Schneider *et al.*, 2013). Episodes of low summer discharges are expected due to longer periods with low precipitation and lower levels of ground water in summer (Hanssen-Bauer *et al*., 2015). The projected changes in temperature and discharge (IPCC 2007), i.e. increased temperatures and changed discharge patterns, may have detrimental effects on aquatic organisms inhabiting rivers because both temperature (Angilletta *et al.*, 2002) and discharge regimes influence important life history traits of many aquatic species, such as growth and mortality (Heino *et al.*, 2009).

The Atlantic salmon life cycle is divided into two phases: the juvenile phase, which takes place in freshwater; and the adult phase, which largely takes place in the ocean. For juvenile salmon in the river, the temperature and discharge pattern are key parameters for survival and growth. The water temperature will affect the speed of physiological and biochemical reactions of this poikilothermic (cold-blooded) organism (Angilletta *et al.*, 2002). Salmon growth is strongly influenced by temperature (Forseth *et al.*, 2001) and size determined by growth is an important factor for juvenile survival (Einum & Fleming, 2007). The stage when juveniles migrate from the river to the ocean as smolts is also largely determined by size (Metcalfe, 1998) and therefore strongly influenced by water temperature. The discharge determines the wetted area of the river, depending on the river profile, with the wetted width of a “U”-shaped cross section changing less with changing discharge than a “V”-shaped cross section. The wetted area of the river controls the river’s carrying capacity, but carrying capacity is also dependent on habitat quality for juvenile salmon, i.e. shelter availability is of great importance (Finstad et al. 2009). The wetted area strongly influences density-dependent

This is the accepted version of an article published in Science of the Total Environment
DOI: 10.1016/j.scitotenv.2018.03.058

mortality in early life-stages, a common bottleneck for salmon abundance in rivers (Einum *et al.*, 2006). Thus, water temperature and discharge drive fundamental biological mechanisms, both at the individual- and population level.

Atlantic salmon has been in a long-term decline in most of its distribution area, both in terms of the number of populations and in terms of abundance in freshwater as well as the marine environment (Hindar *et al*., 2011; Windsor *et al*., 2012; ICES 2013). In Norway, approximately 30% of rivers with salmon stocks are affected by hydropower development, with effects on salmon stocks ranging from extirpation to modest reductions in abundance or even positive effects (Hvidsten *et al.*, 2015). Environmental flow practices in regulated rivers are commonly dominated by a defined constant minimum discharge value for winter and a higher constant value for summer (Alfredsen *et al.*, 2012). These values are often exceeded, but cannot be lower. In a majority of regulated river systems, water masses are commonly stored in reservoirs during periods of high run-off and released in periods when electricity is required, usually in winter. Thus discharge regimes may be adjusted, which often leads to increased winter discharges and reduced spring floods in Norwegian rivers, compared to unregulated rivers. In a few documented cases, hydropower developments have increased smolt abundance in parts of the river (Ugedal *et al*. 2008) or total smolt abundance, in both cases due to increased water discharge during winter (Hvidsten *et al.*, 2015). Active management of river discharge patterns in regulated watercourses may therefore represent a rare case of effective mitigation of negative climate change effects on fish populations (Piou & Prevost, 2013).

The current study explores how the future abundance of Atlantic salmon may be influenced by climate-induced changes in water temperature and discharge in a regulated river, and how negative impacts of climate change may be mitigated by implementing different minimum

This is the accepted version of an article published in Science of the Total Environment
DOI: 10.1016/j.scitotenv.2018.03.058

discharge regimes during critical periods. A spatially-explicit individual-based model is used to predict population abundance under future climate regimes for comparison to abundance under control (past) regimes, with a focus on how the discharge regime affects wetted area and consequently carrying capacity. The effect of climate change on salmonid freshwater abundance has been examined in previous studies (Battin *et al.*, 2007, Hedger *et al.*, 2013b, Leppi *et al.*, 2014), but this is to the authors' knowledge the first study to include minimum discharge regime scenarios, implemented as mitigation strategies for climate change, into the model pathway.

2. MATERIAL AND METHODS

2.1 Study area

The study river, the River Mandalselva (58.2°N, 7.5°E), is one of the largest rivers in southern Norway. The river is 115 km long and is regulated with seven hydropower stations and several reservoirs (Ugedal *et al.*, 2006). Atlantic salmon and brown trout (S*almo trutta* L.) can migrate from the sea 47 km upstream to the natural waterfall of Kavfossen (Fig. 1). The mean discharge at the outlet of the most downstream hydropower station (Laudal) is 88 $m^3 s^{-1}$; average lowest daily discharges range between 18.6 $m^3 s^{-1}$ during summer (Jul-Sep) and 33.1 $m^3 s^{-1}$ during winter (Jan-Mar) (Ugedal *et al*., 2006). The Mandal system has a total storage capacity of 358 million m^3 (NVE Atlas, https://atlas.nve.no), providing the opportunity to store water from extra winter precipitation and to release this water in drier periods of the year.

This is the accepted version of an article published in Science of the Total Environment
DOI: 10.1016/j.scitotenv.2018.03.058

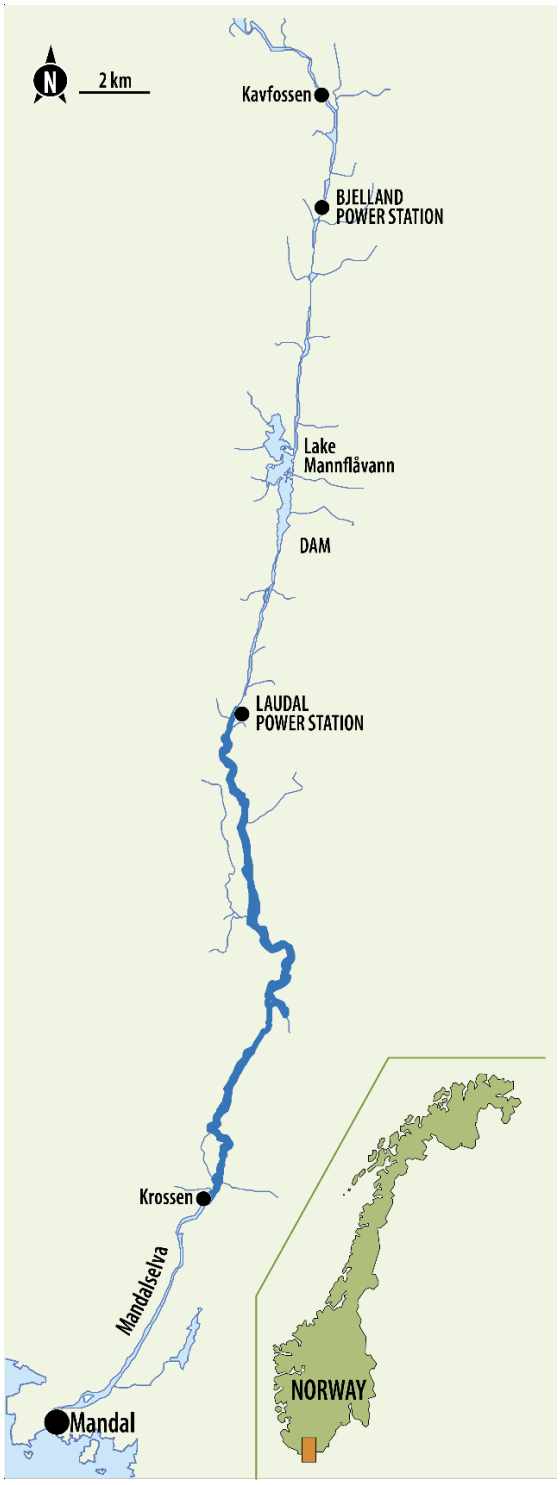

Fig. 1. River Mandalselva with the modelled stretch of the river marked with a thick blue line, from the outlet of Laudal Power station and downstream to Krossen (start of the tidal zone).

This is the accepted version of an article published in Science of the Total Environment
DOI: 10.1016/j.scitotenv.2018.03.058

In the beginning of the 20th century, the salmon fisheries in the river were highly productive, but acidification during the 1960s extirpated the original salmon population. However, liming was initiated in 1997 and a new salmon stock, resulting from strayers from other rivers and the release of eggs and fry from a stock in a nearby river, rapidly increased in size. The catch peaked at 10 tonnes in 2001. The present salmon stock in the river is a genetic blend, with likely weak or no links to the original stock (Hesthagen *et al.*, 2010).

2.2 Modelling procedure

Water temperature and discharge (and consequently wetted area) in the regulated stretch downstream of the Laudal hydropower station – stretching downstream 20 km from the outlet of the station (upstream distance = 20.5 km) to the start of the tidal zone (upstream distance = 700 m – were generated for selected climate scenarios using a modelling hierarchy (Fig. 2). Coarse-scale predictions of air temperature and precipitation from Global Climate Models (GCMs) were downscaled using a Regional Climate Model (RCM) to provide finer-scale predictions (spatial resolution = 1 km^2) of air temperature and precipitation across the catchment encompassing the Mandalselva. These data were used to determine the hydrological regime of the catchment using a hydrological model. Given that the Mandalselva is regulated and the hydraulic properties of the river are influenced by hydropower operation as well as the hydrological regime, outputs from the hydrological model were used in a hydropower production model, to provide water temperature and discharge. A hydraulic model was then used to derive weekly wetted area, a critical component of the individual-based population model, from the discharge data.

This is the accepted version of an article published in Science of the Total Environment
DOI: 10.1016/j.scitotenv.2018.03.058

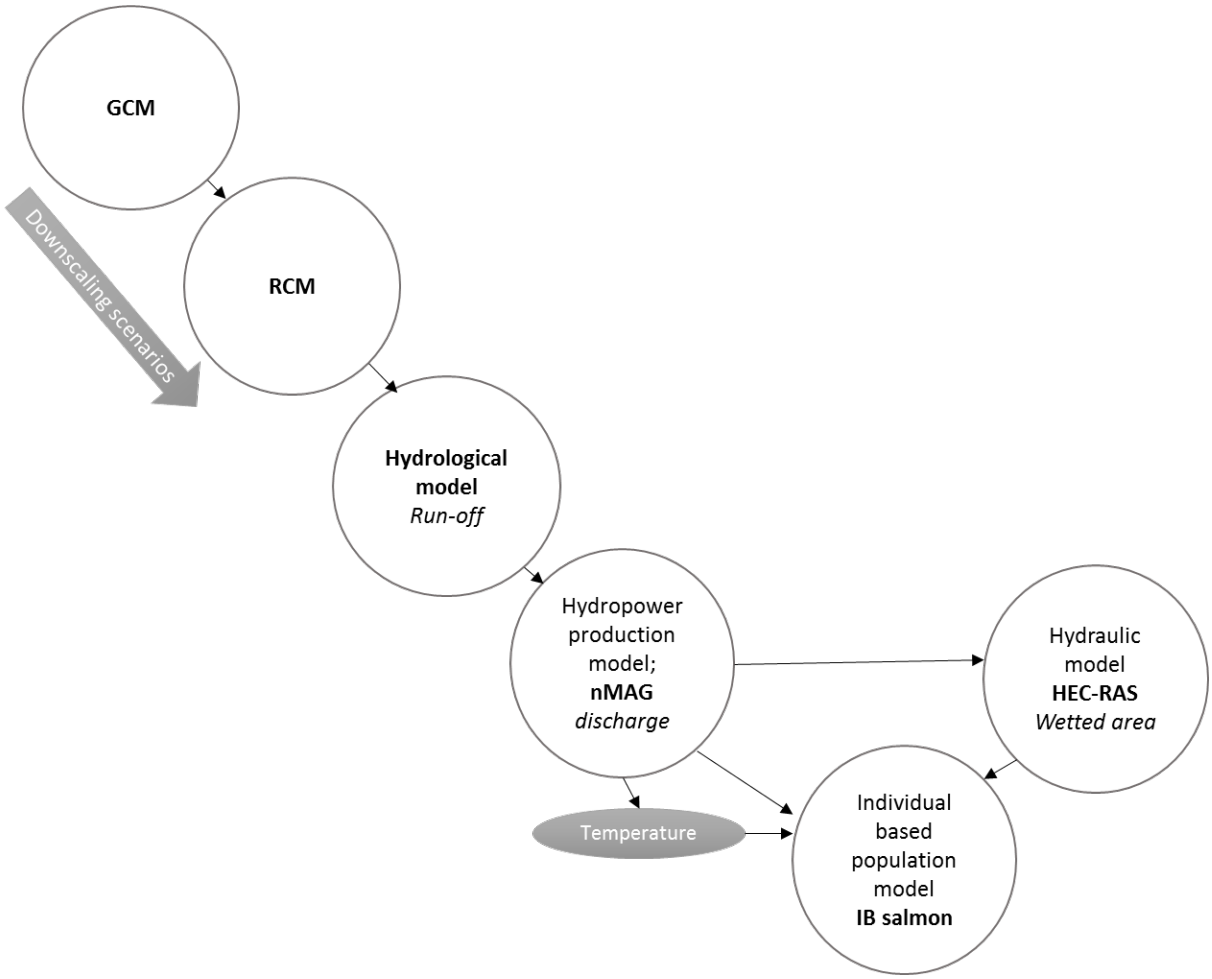

143

144 **Fig. 2. The model pathway from downscaling of the Global Climate Model (GCM), via a**
145 **Regional Climate Model (RCM), to hydrological-, hydropower- and hydraulic- models,**
146 **and finally down to the individual-based population model, IB-salmon.**

147

148 **2.3 Global Climate Model (GCM) and Regional Climate Model (RCM)**

149 Climate data used in this study were provided by the Norwegian Meteorological Institute
150 DNMI (Engen-Skaugen *et al*., 2008). These data were derived from predictions from the
151 Hadley Centre's HadAm3H GCM and the Max Plank Institute's ECHAM4 GCM. Scenarios
152 used were both for (1) future climates, the SRS A2 (high CO_2) and B2 (low to medium CO_2)
153 emission scenarios (2071-2100), and (2) a control climate, SRS CN (1960-1990) (Table 1).

This is the accepted version of an article published in Science of the Total Environment
DOI: 10.1016/j.scitotenv.2018.03.058

These scenarios are used by the DNMI to evaluate the future climate in Norway. The SRS A2 and B2 emission scenarios are described in the IPCC Fourth Assessment Report (IPCC 2007) and represent the climate forcing through CO_2 emissions for specific scenarios of future development of the world (IPCC SRES 2000), and are respectively similar to the RCP 8.5 and RCP 6.0 scenarios used in the IPCC Fifth Assessment Report (IPCC 2014) (see van Vuuren & Carter, 2014). GCM data were at a 55 × 55 km regional domain (spatial resolution) for the HadAm3H model, and at both this domain and a finer domain (25 × 25 km) for the ECHAM4 model. GCM predictions of temperature and precipitation were then downscaled to a finer resolution (grid of 1 km^2 cells) by the DNMI using the Regional Climate Model (RGM) HIRHAM (Christensen et al. 2007; May 2007) which was bias adjusted based on observations of local climate (Engen-Skaugen, 2007). The use of data from different GCMs with different spatial domains allowed the investigation of how prone predictions of salmon population abundance were to the climate model outputs on which the analyses were based.

This is the accepted version of an article published in Science of the Total Environment
DOI: 10.1016/j.scitotenv.2018.03.058

Table 1. Overview of Global Climate Models (GCM), emission scenarios, spatial resolutions of GCM output data, and scenarios simulations used with the individual-based model (IBM).

GCM	Emission scenario	Domain	Spatial resolution (km)	IBM scenario name
HadAm3H	A2 + control	RegClim	55 × 55	Had.Reg.A2
				Had.Reg.CN
HadAm3H	B2 + control	RegClim	55 × 55	Had.Reg.B2
				Had.Reg.CN
ECHAM4	B2 + control	RegClim	55 × 55	ECHAM.Reg.B2
				ECHAM.Reg.CN
ECHAM4	B2 + control	NorAcia/NorClim	25 × 25	ECHAM.Nor.B2
				ECHAM.Nor.CN

2.4 Hydrological model

Downscaled temperature and precipitation predictions from the RCM were used as input to a hydrological model to predict water inflows along the complete watercourse of the Mandalselva. Hydrological modelling was performed in the open source model platform ENKI (Kolberg & Bruland, 2012). This gridded model simulates inflow based on meteorological inputs (temperature and precipitation) and catchment characteristics (elevation, soil water storage, distribution of sub-catchments and river network). The model

This is the accepted version of an article published in Science of the Total Environment
DOI: 10.1016/j.scitotenv.2018.03.058

interpolates temperature and precipitation across the catchment using Inverse-Distance Weighting and Kriging, respectively. Soil-moisture and surface runoff (from excess soil moisture) are then calculated using the response function developed for the Hydrologiska Byråns Vattenbalanavdeling (HBV) model. To achieve a better model of soil moisture and surface runoff, the model includes an evaporation routine based on the routine in LandPine model (Rinde, 2000) and a snow accumulation/snowmelt routine (see Kolberg *et al.*, 2006). The former reduces soil moisture and runoff (particularly in the summer); the latter introduces a lag in soil moisture and runoff by storing precipitation as snow during winter, and releasing this in spring. The model is calibrated for individual sub-catchments within the entire catchment by setting the model to run for one individual sub-catchment at a time and validating with the remaining catchments (iterating with the Shuffled Complex Evolution Method, with Nash Sutcliffe's efficiency criteria (Nash & Sutcliff, 1970)).

2.5 Hydropower production model

The hydropower production discharge in the river was simulated using the nMAG model (Killingtveit & Sælthun, 1995; Killingtveit, 2004) based on inputs from the hydrological model. The nMAG model simulates hydropower operations for whole systems consisting of hydropower stations, reservoirs and transfers, and predicts river discharge among other variables. A model of the hydropower system with all reservoirs and power stations in the Mandalselva was used (Fjeldstad *et al.*, 2014) and the operational strategy of the power system was kept unchanged among the climate scenarios. Water temperature downstream of the Laudal hydropower system was found from regression equations based on observed water temperature, air temperature, production discharge and simulated inflow. Water temperature

This is the accepted version of an article published in Science of the Total Environment
DOI: 10.1016/j.scitotenv.2018.03.058

202 in the modelled watercourse, T_w, was calculated by weighting the temperature contributions
203 from natural inflow and the reservoir immediately upstream (Equation 1):

$$T_w = \frac{Q_{in}}{Q_{tot}} T_{in} + \frac{Q_{res}}{Q_{tot}} T_{res} \quad (1)$$

204 where T_{in} and T_{res} are water temperatures from natural inflow and the reservoir respectively,
205 Q_{in} and Q_{res} are the respective discharges, and Q_{tot} is the total discharge. Water temperatures
206 in the natural inflow and in the reservoir were estimated from regression relationships
207 established with air temperature, T_a (Equation 2 and 3).

$$\begin{cases} T_{in} = 0.5 & T_a < -3 \\ T_{in} = 0.0658{T_a}^2 + 0.5287T_a + 1.5707 & -3 \geq T_a \leq 1 \\ T_{in} = 0.9567T_a - 0.8926 & T_a > 1 \end{cases} \quad (2)$$

208

$$\begin{cases} T_{res} = 0.13 & T_a < -6 \\ T_{res} = 0.0567{T_a}^2 + 0.5117T_a + 1.5617 & -6 \geq T_a \leq 1 \\ T_{res} = 1.0324T_a + 1.1685 & T_a > 1 \end{cases} \quad (3)$$

209

210 **2.6 Hydraulic model**

211 In order to estimate the relationship between discharge and wetted area in the modelled
212 stretch, the HEC-RAS® (2008) hydraulic model was applied. This model can simulate
213 discharges within rivers, for both steady-flow surface profiles, and 1-D and 2-D unsteady flow
214 conditions. The HEC-RAS model was used to determine discharge – wetted width
215 relationships for each of three stations with different channel profile characteristics
216 representative of the modelled stretch of the river: channel profiles were more "U"-shaped,
217 more "V" shaped, and intermediate between these two. The model was calibrated with field

This is the accepted version of an article published in Science of the Total Environment
DOI: 10.1016/j.scitotenv.2018.03.058

observations of water level measurements in each station at a single discharge by varying the Manning's roughness coefficient (0.020 – 0.095) until the model prediction matched field observations. 1-D steady-state simulations were then performed at various discharges to establish discharge – wetted width curves (Fig 3a). Curves were extrapolated for discharges outside of the validated discharge range of the HEC-RAS simulations. The discharge – wetted width curves of the three stations were then transferred to the 50 m long river sections with corresponding channel profiles (determined by aerial photography) and scaled by the ratio between the maximum wetted width of the 50 m section in question (again, determined by aerial photography) and the maximum wetted width of the respective station. This enabled the estimation of the discharge – wetted width relationship for each section throughout the entire modelled stretch of the river. The wetted area of each section was calculated by multiplying the section wetted width by the section wetted length (50 m), giving a highly non-linear relationship between discharge and total wetted area in the modelled watercourse (Fig 3b).

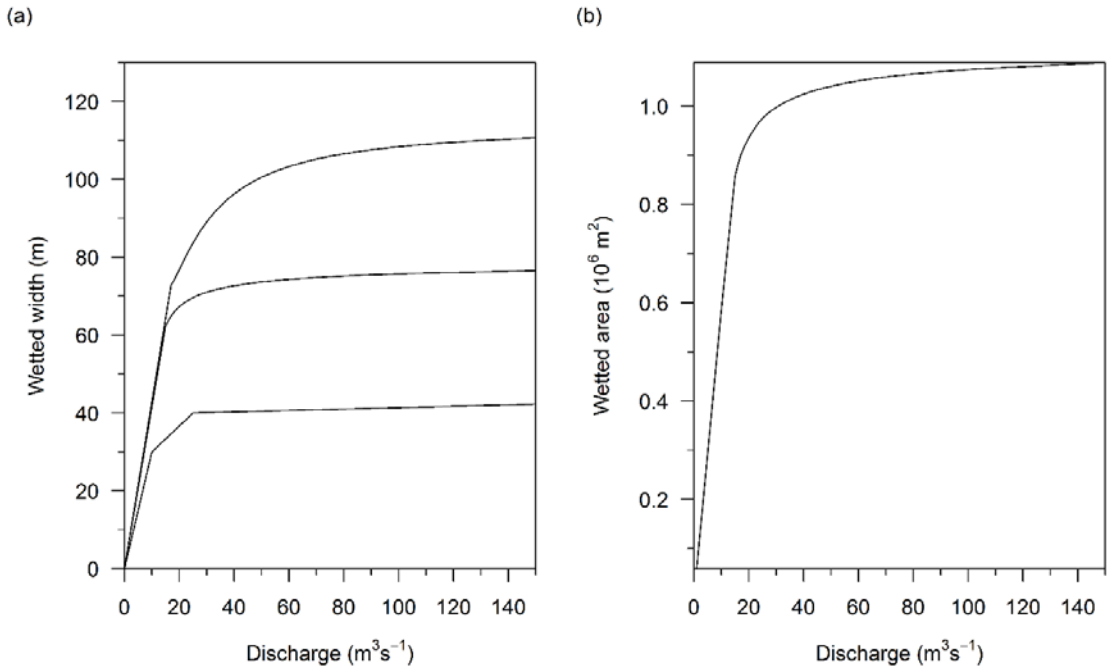

Fig. 3. Relationship between discharge and (a) wetted width in the HEC-RAS stations, and (b) total wetted area in the modelled watercourse.

This is the accepted version of an article published in Science of the Total Environment
DOI: 10.1016/j.scitotenv.2018.03.058

2.7 Atlantic salmon population model

An individual-based modelling (IBM) approach was used to predict the impact of climate change and mitigation measures on population abundances (expressed in this study as total number of individuals within the modelled stretch) and changes in life history characteristics of Atlantic salmon within the modelled watercourse. This approach was used because several aspects of the processes affecting the salmon population would have been difficult to parameterize using population differential equations (see DeAngelis and Grimm, 2014). For example, changes in mortality resulted from changes in wetted area, which operate at a spatially local level. Local changes in wetted area depend on local carrying capacity, local river profile, local habitat quality and local parr biomass, and also the spatial configuration of different carrying capacities, channel widths and biomass. Running an IBM allowed population characteristics to dynamically emerge from heuristic functions that were well parameterized at the spatially local and individual level.

Model functions

The IBM used (IB-salmon) (Hedger *et al.*, 2013a, Hedger *et al.*, 2013b; Sauterleute *et al.*, 2016) is a spatially-explicit model designed for predicting population characteristics of the freshwater stage of juvenile Atlantic salmon, but also models sea survival and the return of surviving adults from the sea. The model has a time-step interval of one week, with the river divided into a series of 50 m sections. Individual life-history traits (growth, smoltification timing, fecundity, mortality) and other characteristics (location, migration) are modelled using empirical functions (Hedger *et al.*, 2013a, Hedger *et al.*, 2013b). Life-stages modelled as individual elements are parr (juveniles in the river), smolts (parr that have smoltified, which then migrate to sea), sea resident adults, and returning adults (adults that have returned to the

This is the accepted version of an article published in Science of the Total Environment
DOI: 10.1016/j.scitotenv.2018.03.058

river to spawn). The main input parameters of the model are wetted area (dependent on channel profile and discharge), water temperature, spawning location and area, and parr carrying capacity. At the beginning of a simulation, annual egg deposition is read from a file, and binned into sections according to relative spawning habitat quality. Later when a full age-distribution of spawning adults has returned, eggs are deposited in sections as a function of spawning female abundance and body mass in which the spawning female was born. The weekly parr growth is determined using a Ratkowsky-type model (Ratkowsky *et al.*, 1983) parameterized with experimental data on growth/temperature relationships for Norwegian Atlantic salmon juveniles (Jonsson *et al.*, 2001) (Equation 4).

$$\begin{cases} M_t = M_{t-1} & T < \mathrm{T_L} \text{ or } \mathrm{T} > \mathrm{T_U} \\ M_t = \left(M_{t-1}^b + b\left(\dfrac{d(T - \mathrm{T_L})\left(1 - e^{g(T - \mathrm{T_U})}\right)}{100} \right) \right)^{(1/b)} & T \geq \mathrm{T_U} \;\&\; T \leq \mathrm{T_U} \end{cases} \quad (4)$$

where M is the individual body mass for time t, T is the weekly mean temperature, $\mathrm{T_L}$ and $\mathrm{T_U}$ are lower and upper temperatures for growth, and b, d and g are parameters of the model.

Body length, L, is predicted from body mass every week, using a power function relationship (Equation 5).

$$L = \left(10^5 M / 0.84\right)^{1/3} \quad (5)$$

The annual smoltification probability (applied in week of year 20), SP, is estimated for each individual as a logistic function of body length, L (Equation 6).

This is the accepted version of an article published in Science of the Total Environment
DOI: 10.1016/j.scitotenv.2018.03.058

$$\begin{cases} SP = \dfrac{e^{(p1+(p2\times L))}}{1+e^{(p1+(p2\times L))}} & if\ L \leq 250 \\ SP = 1 & if\ L > 250 \end{cases} \quad (6)$$

where $p1$ and $p2$ are parameters of the model.

Parr density dependent mortality in any given section is dependent on the total biomass of parr within that section (the sum of individual body masses of all parr in the section) and the total carrying capacity of the section (the total biomass that can be supported, which is the product of the carrying capacity per unit area and the total wetted area of the section). If the biomass within a section exceeds the total carrying capacity, surplus parr are forced to migrate out of the section: they may either migrate to a new section or experience mortality (density dependent mortality) (Equation 7).

$$\begin{cases} B_{s,t} = B_{s,t-1} & B_{s,t-1} < \mathrm{K} \\ D_{s,t} = \mathrm{s}\left(B_{s,t} - \mathrm{K}\right) & B_{s,t-1} \geq \mathrm{K} \\ B_{s,t} = \mathrm{K} + D_{s+1,t-1} & \end{cases} \quad (7)$$

where B is the total parr biomass (g m^{-2}) within the section, s, at time, t, D is the total parr biomass (g m^{-2}) of individuals that disperse out of the section and survive, K is parr carrying capacity (g m^{-2}) and s is the parr survival probability. Density dependent mortality may increase if the section biomass increases (due to body mass growth or an increase in abundance via recruitment or immigration) or the total carrying capacity of the section decreases due to a decrease in the wetted area.

Parameterizing and running the model in the Mandalselva

The model was parameterized to run on a part of the river stretching 20 km downstream from the outlet of the most downstream hydropower station (Fig. 1). Discharge into this stretch of the river is regulated by the hydropower operator: with water entering from a turbine output

This is the accepted version of an article published in Science of the Total Environment
DOI: 10.1016/j.scitotenv.2018.03.058

and from an upstream bypass (minimum discharges of 3 m s^{-1} and 1.5 m s^{-1} in summer and winter respectively). The minimum discharge was manipulated in future scenarios to study the effect of mitigation measures. The model was parametrized and validated using available data on electrofishing juvenile densities (Fig. 4) and juvenile size at age (based on electrofishing at seven stations in October/ November, yearly from 2002 – 2010, Norwegian Environment Agency), and smolt abundance at age (see Ugedal et al. 2006). Habitat quality of each section in the modelled stretch was based on field surveys of substrate type and size, spawning habitat and shelter measurements (Finstad et al. 2007). Spawning habitat was determined from survey data. A spawning habitat quality index, varying between zero (no spawning) and one (maximum spawning), was used to allocate the initial egg deposition at start of simulations to the different sections.

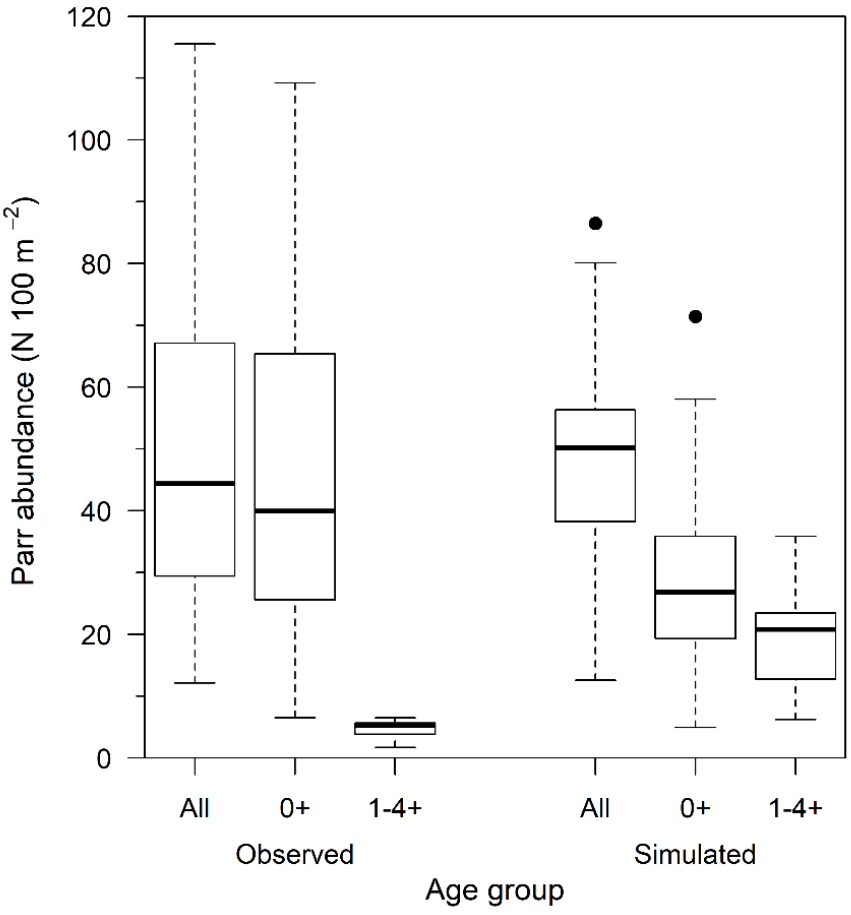

This is the accepted version of an article published in Science of the Total Environment
DOI: 10.1016/j.scitotenv.2018.03.058

Fig. 4. Observed parr abundance and age distribution from electrofishing juvenile densities compared to simulated parr abundance and age distribution from the salmon abundance model (IB salmon).

The model was run with a "burn-in" time of 10 years to allow for the simulation of a salmon population, followed by 40 years of simulation to provide output data on the population. The burn-in-time is used to create stable population processes (see Williams *et al.*, 2017) – in the case of IB-salmon, this involved generating an age- and size-specific population distribution from an initial estimate of egg deposition. Predictions from the burn-in time were excluded from the analysis. For analysis of the effect of changes in climate scenarios and discharge regimes on population abundance, one population was simulated per set of parameter values.

Given that the IBM included probabilistic functions, generated populations abundances would vary according to simulation, even with the same set of parameter values. However, a preliminary analysis of simulations showed that the effect of stochasticity in generated output was small. For example, when running ten separate simulations for each of the climate scenarios, the coefficient of variation (CV) for annual smolt abundance was always less than 0.2% for each climate scenario. This CV was negligible in comparison to the difference in smolt abundance between different climate scenarios.

2.8 Mitigation in future climates

In order to explore potential mitigation measures for climate change and how these would affect juvenile abundance, simulations were run with the implementation of minimum discharge regimes during summer weeks (week 20-40). Summer discharges in most future scenarios were less than those of the corresponding control scenarios (see Table 2). Therefore,

This is the accepted version of an article published in Science of the Total Environment
DOI: 10.1016/j.scitotenv.2018.03.058

regulating discharges so that they were greater than what would occur naturally during this period allowed for comparing potential mitigation measures for climate change. Five summertime minimum discharge regimes were examined: 2, 4, 6, 8 and 10 $m^3 s^{-1}$. These minimum discharge regimes are sustainable from the high storage capacity of the Mandalselva system.

This is the accepted version of an article published in Science of the Total Environment
DOI: 10.1016/j.scitotenv.2018.03.058

Table 2. The summary statistics (median, min, max and range) of discharge (m^3s^{-1}) in control (1961-1990) and future scenarios (2070-2100), for all years and for the summer period (week 20-40).

	All year				Summer period (week 20-40)			
Scenarios	**Median**	**Min**	**Max**	**Range**	**Median**	**Min**	**Max**	**Range**
Control (1961-1990)	64.6	2.4	445.0	442.6	53.1	2.4	260.0	257.6
	67.7	1.8	490.0	488.2	52.4	1.8	311.3	309.6
	66.4	2.4	462.5	460.1	55.0	2.4	267.2	264.8
Future (2070-2100)	61.37	0.61	347.5	346.9	12.5	0.6	116.5	115.9
	60.33	1.5	521.83	520.33	18.5	1.5	197.6	196.1
	75.03	3.08	499.21	496.13	38.4	3.1	374.8	371.7
	64.84	1.08	390.41	389.33	21.5	1.1	198.2	197.1

3. RESULTS

3.1 Climate change in future scenarios

3.1.2 Hydraulic predictions

Water temperature increased under all future scenarios (Had.Reg.A2, Had.Reg.B2, ECHAM.Reg.B2 and ECHAM.Nor.B2) compared to the control scenarios (Fig. 5, Table 3). The Had.Reg.B2 scenario showed a slightly lower mean temperature during summer weeks than the Had.Reg.A2 scenario, but one that was still several degrees higher than the control scenario.

This is the accepted version of an article published in Science of the Total Environment
DOI: 10.1016/j.scitotenv.2018.03.058

344 **Table 3. Mean water temperatures** (°C) **in the control (1961-1991) and future climate**

345 **scenarios (2071-2100).**

Scenarios	Global circulation models	Temperature (°C)
Control	Had.Reg.CN	6.25 (SD ± 5.16)
Control	ECHAM.Reg.CN	6.27 (SD ± 5.16)
Control	ECHAM.Nor.CN	6.27 (SD ± 5.14)
Future	Had.Reg.A2	9.05 (SD ± 5.76)
Future	Had.Reg.B2	8.48 (SD ± 5.52)
Future	ECHAM.Reg.B2	8.66 (SD ± 5.76)
Future	ECHAM.Nor.B2	8.89 (SD ± 5.16)

346

This is the accepted version of an article published in Science of the Total Environment
DOI: 10.1016/j.scitotenv.2018.03.058

Winter discharges in all future scenarios were greater than in the corresponding control scenarios. In contrast, the spring flood was reduced in all future scenarios compared to the control, and occurred a few weeks earlier in the year. Discharges in the summer months of June, July and August were lower in the future scenarios than in the control scenarios (Fig. 5). Of the future scenarios, the ECHAM.Reg.B2 scenario predicted a higher discharge in summer than the future Had.Reg.A2, Had.Reg.B2 and ECHAM.Nor.B2 scenarios.

In summer, wetted area was considerably reduced in the future scenarios Had.Reg.A2, Had.Reg.B2 and ECHAM.Nor.B2. In contrast, wetted area predicted under the ECHAM.Reg.B2 scenario, did not change considerably compared to the control scenario. (Fig. 5).

This is the accepted version of an article published in Science of the Total Environment
DOI: 10.1016/j.scitotenv.2018.03.058

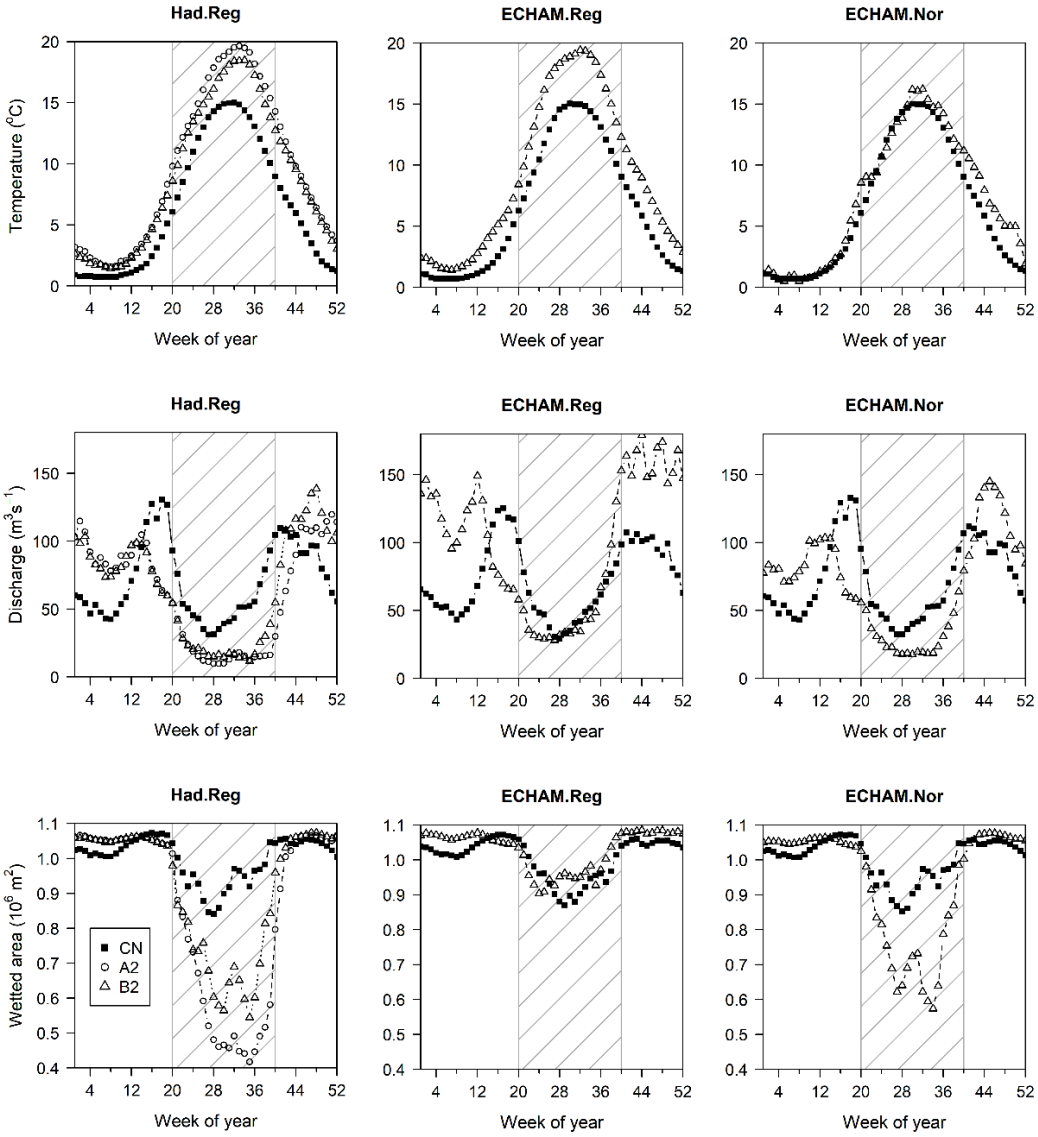

358

359 **Fig. 5. Modelled mean weekly water temperature, discharge and wetted area in the**
360 **control (1961-1991) and future (2071-2100) scenarios. Curves show mean weekly values**
361 **across all output years of the simulation: control scenarios (filled squares); A2 scenarios**
362 **(circles); and B2 scenarios (triangles). Hatched areas show the summer season.**

363

This is the accepted version of an article published in Science of the Total Environment
DOI: 10.1016/j.scitotenv.2018.03.058

3.1.2 Salmon population predictions

Parr abundance decreased in all future scenarios, compared to the respective control scenarios (Fig. 6 a). This reduction was, however, small in the ECHAM.Reg.B2 scenario. Because of changes in age at smoltification and subsequent emigration to sea, the age composition in all future scenarios shifted towards younger parr in comparison to the control scenarios. In the future scenarios, the 3+ and 4+ juvenile age class (in years) disappeared and a very small proportion of 2+ was left, compared to the control scenarios.

Smolt abundance in three of the future scenarios – Had.Reg.A2, Had.Reg.B2 and ECHAM.Nor.B2 – was less than in the respective control scenarios (Fig. 6 b). However, smolt abundance in the ECHAM.Reg.B2 scenario was greater than in the respective control scenario. The age composition of smolts changed in all future scenarios, with age shifting towards a year younger compared to smolts in the control scenarios. The majority of smolts in the future scenarios were 2+, compared to 3+ and 4+ in the control scenarios.

The weekly density dependent mortality of parr (as a proportion of the total parr abundance) was inversely correlated with wetted area and was highest during the summer period in all future climate scenarios, when the wetted area was predicted to be small (Fig. 7). Future scenarios with greater summertime reduction in wetted area (HAD scenarios) caused greater density dependent mortality than scenarios with smaller summertime reductions in wetted area (ECHAM scenarios).

This is the accepted version of an article published in Science of the Total Environment
DOI: 10.1016/j.scitotenv.2018.03.058

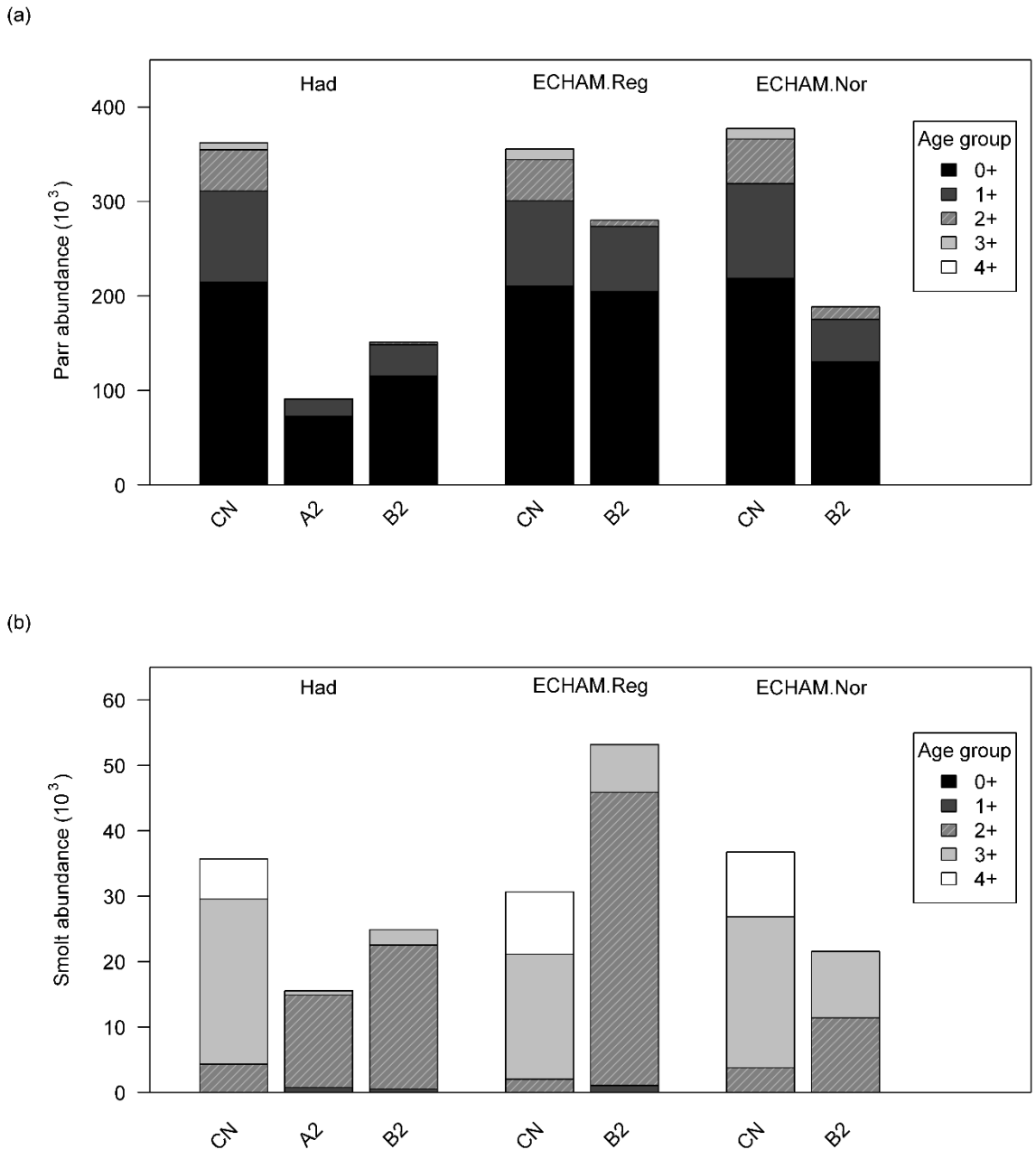

383

384 **Fig. 6. Mean parr abundance (a) and smolt abundance (b) according to age (0+, 1+, 2+,**

385 **3+, 4+) in the control (1961-1991) and future (2071-2100) scenarios.**

This is the accepted version of an article published in Science of the Total Environment
DOI: 10.1016/j.scitotenv.2018.03.058

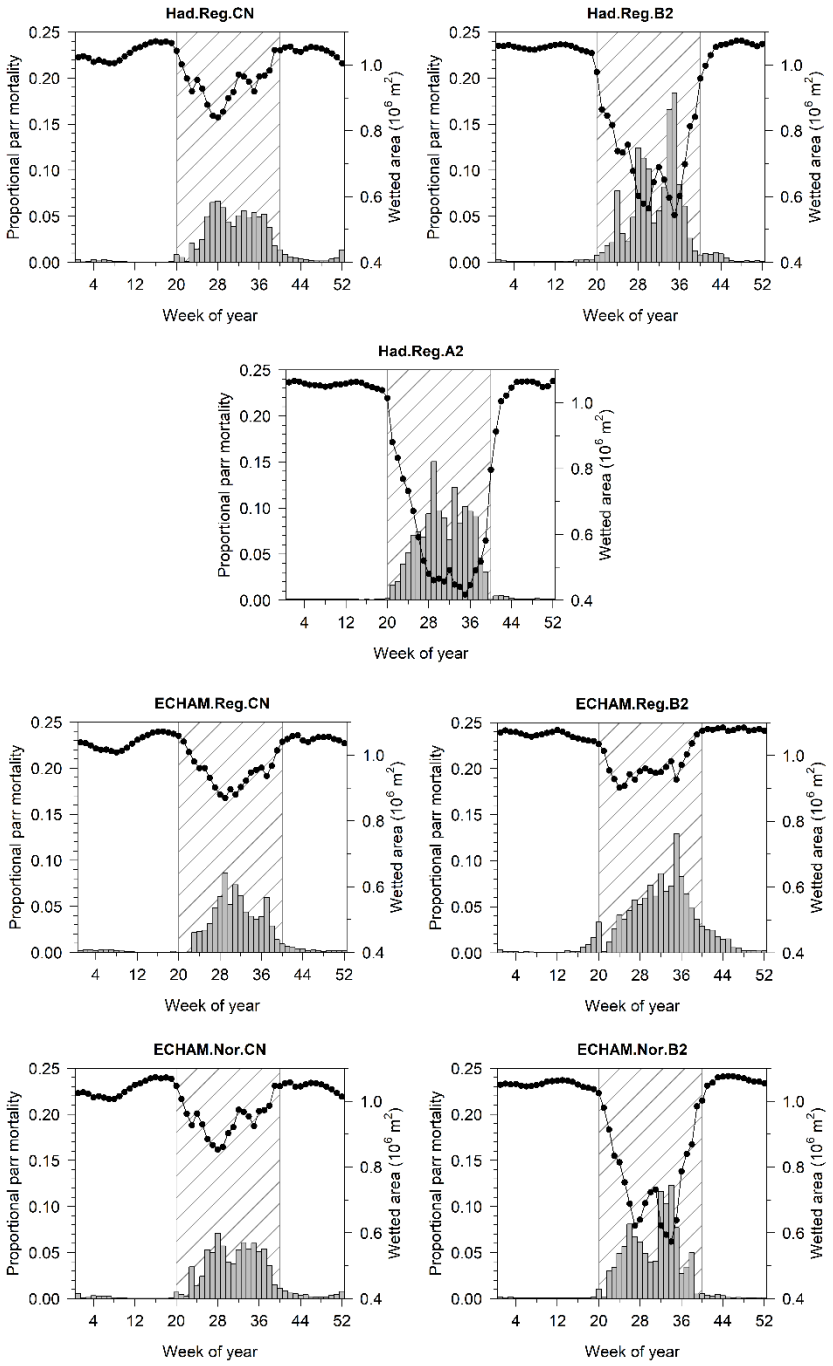

386

387 **Fig. 7. Mean weekly density dependent mortality of parr (proportion of the total weekly**
388 **parr abundance) and the corresponding weekly wetted area in the control (1961-1990)**
389 **and future (2071-2100) scenarios. Barplots and curves show mean weekly values across**
390 **all output years of the simulation. Hatched areas show the summer season.**

391

This is the accepted version of an article published in Science of the Total Environment
DOI: 10.1016/j.scitotenv.2018.03.058

3.2 Mitigation of climate change

3.2.1 Discharge and wetted area

Discharges in the future scenarios were reduced during summer weeks, particularly in projection Had.Reg.A2, Had.Reg.B2 and ECHAM.Nor.B2, and less so in the ECHAM.Reg.B2 scenario. Implementation of minimum discharge regimes (from 2 to 10 $m^3 s^{-1}$) increased summer wetted area for the Had.Reg.A2, Had.Reg.B2 and ECHAM.Nor.B2 scenarios (Fig. 8). The effect was strongest for the Had.Reg.A2 where summer wetted areas increased from $\approx 4.5 \times 10^6$ m^2 under conditions of no assigned minimum discharge to $\approx 7 \times 10^6$ m^2 under a minimum discharge of 10 m s^{-1}. In contrast, implementation of minimum discharge regimes had little effect on wetted areas for the ECHAM.Reg.B2 scenario during summer months due to summer discharges in this scenario being greater than those assigned in the minimum discharge regimes.

3.2.2 Parr and smolt abundance

When running the IBM with a range of different minimum discharge regimes, parr and smolt abundance increased with increasing minimum discharge in all scenarios except for the ECHAM.Reg.B2 scenario (Fig. 9). The increase in abundance of both parr and smolt occurred when minimum discharge in summer was 4 $m^3 s^{-1}$ or greater. The ECHAM.Reg.B2 scenario was not strongly influenced by the different minimum discharge regimes because the predicted discharge in summer was higher than that assigned in the minimum regimes.

This is the accepted version of an article published in Science of the Total Environment
DOI: 10.1016/j.scitotenv.2018.03.058

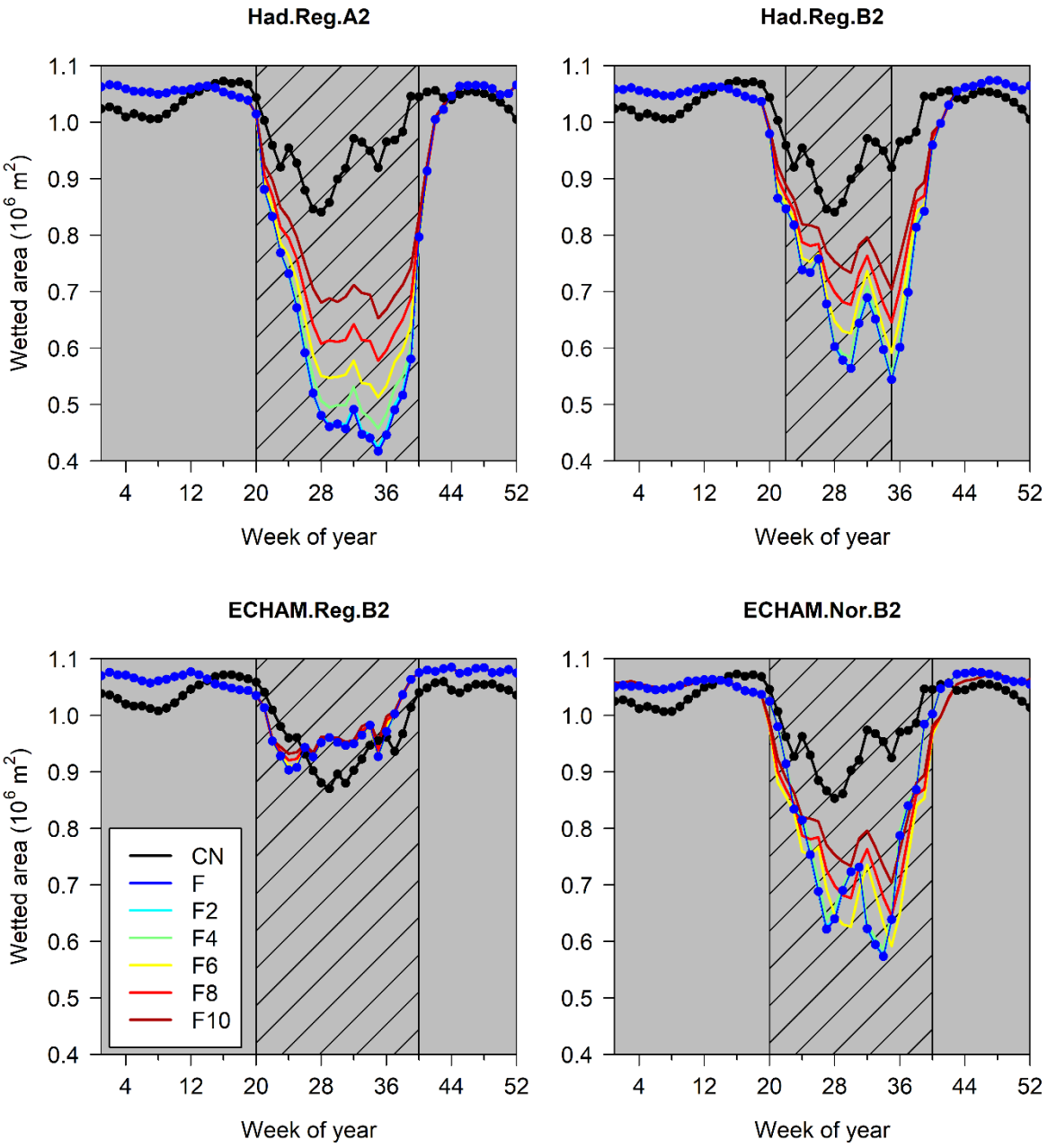

411

412 **Fig.8. Mean weekly wetted area in the control (1961-1990) and future (2071-2100)**
413 **scenarios with a minimum discharge in week of year 20 - 40 of 2, 4, 6, 8 and 10 m^3s^{-1} in**
414 **the future scenarios. Curves show mean weekly values across all output years of the**
415 **simulation. Hatched areas show the summer season.**

This is the accepted version of an article published in Science of the Total Environment
DOI: 10.1016/j.scitotenv.2018.03.058

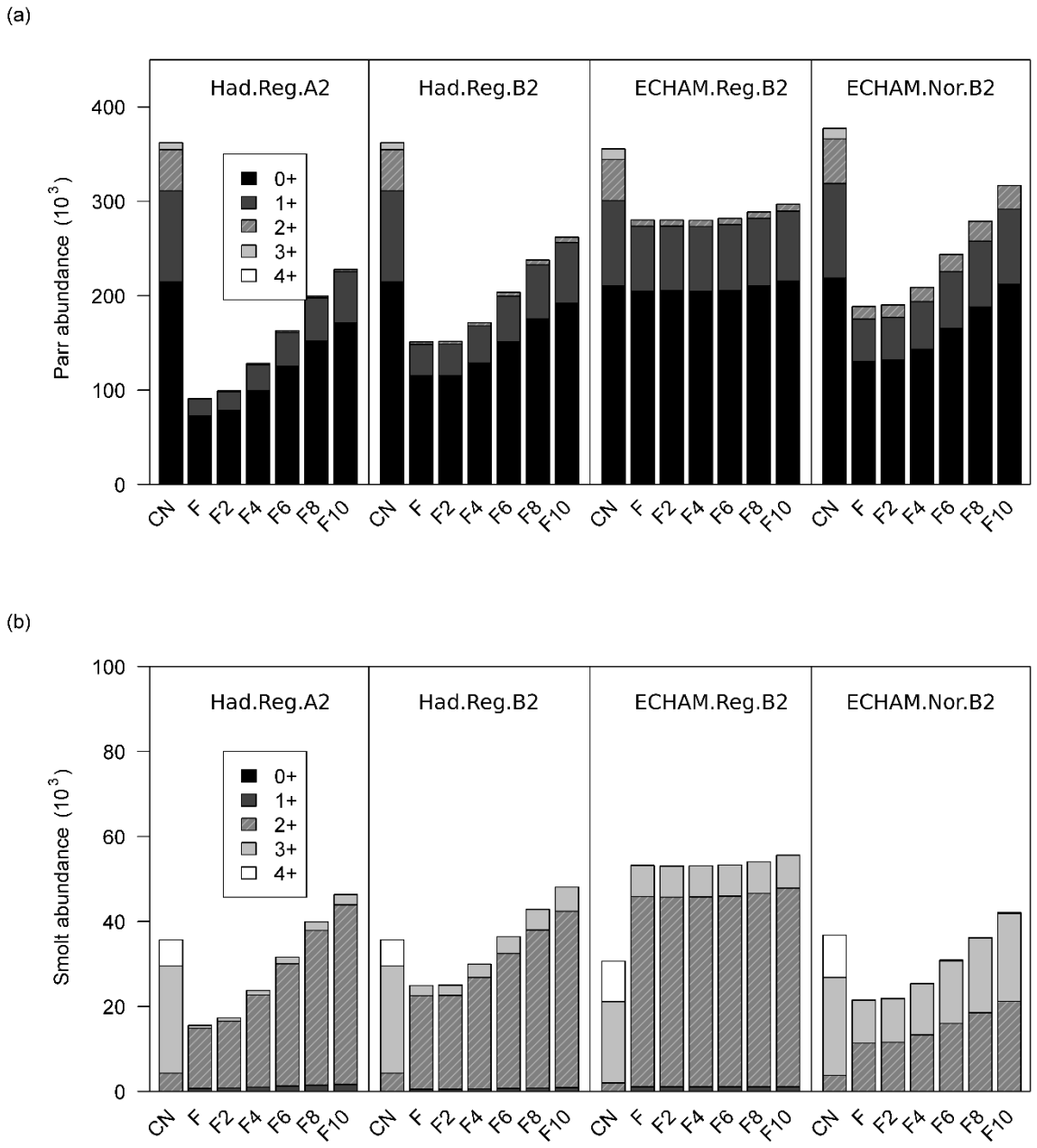

Fig. 9. Mean parr abundance (a) and smolt abundance (b) according to age (0+, 1+, 2+, 3+, 4+) in the control (1961-1990) and future (2071-2100) scenarios, with a minimum discharge in week 20-40 of 2, 4, 6, 8 and 10 m^3s^{-1} in the future scenarios.

This is the accepted version of an article published in Science of the Total Environment
DOI: 10.1016/j.scitotenv.2018.03.058

4. DISCUSSION

4.1 Effect of climate scenarios on future freshwater salmon abundance

In this study, the effect of future climate change on an Atlantic salmon population in a regulated river was modelled, and bottlenecks for salmon abundance in future climates were identified. This study suggests that the abundance of Atlantic salmon in future climates will decrease for the region modelled, and elucidates mechanisms important for regulation of juvenile Atlantic salmon individuals. Low water discharge in summer was identified as a possible bottleneck, and simulation of different minimum discharge regimes showed that changes in river regulation may be a possible mitigation measure. The exact change in Atlantic salmon abundance depended on the GCM and GCM domain used to supply predictions of air temperature and precipitation, so further advances in GCM modelling are required to increase the robustness of the prediction of how any given Atlantic salmon population will respond to climate change.

Reduced parr abundance was found in all future climate scenarios in comparison to control scenarios, although the reduction was small for the ECHAM.Reg.B2 scenario. Three out of four climate scenarios (Had.Reg.A2, Had.Reg.B2 and ECHAM.Nor.B2) predicted reduced smolt abundance, whereas the fourth (ECHAM.Reg.B2) predicted increased smolt abundance. Climate outputs derived from the three climate scenarios – Had.Reg.A2, Had.Reg.B2 and ECHAM.Nor.B2 – resulted in a strong reduction in wetted area during summer relative to the respective control scenarios. Reduced wetted areas during summer caused increased density-dependent mortality of juveniles, resulting in low parr abundances and reduced abundance of smolts. In contrast, climate outputs from the ECHAM.Reg.B2 climate scenario resulted in little change in summer-wetted area compared to the control scenario and consequently little change in density dependent mortality. The model results therefore suggest that wetted area,

This is the accepted version of an article published in Science of the Total Environment
DOI: 10.1016/j.scitotenv.2018.03.058

446 particularly during the summer months, regulates salmon abundance in the Mandalselva,
447 where long periods during summer with low discharge will represent a bottleneck for future
448 salmon abundance by increasing density dependent mortality. This result is consistent with
449 other studies, which have found discharge to be one of the most important factors regulating
450 the freshwater abundance of Atlantic salmon (Gibson & Myers, 1988; Ugedal *et al*., 2008).
451 For example, Hvidsten *et al.* (2015) analysed field data of Atlantic salmon juvenile densities
452 and discharges from a 27 year time series and found that low discharges during both summer
453 and winter affected smolt abundance negatively. However, increased discharges in a future
454 climate may in other locations reduce salmon survival and future peak flows may increase
455 egg-to-fry mortality (Leppi et al. 2014).

456

457 "However, increased discharges in a future climate may in other locations reduce salmon
458 survival and future peak flows may increase egg-to-fry mortality

459 Parr abundance decreased in the ECHAM.Reg.B2 scenario compared to the control scenario,
460 but smolt abundances were still higher than in the control scenario. This can be explained by a
461 higher annual turnover of parr to smolt in the future scenarios. Age of smoltification is linked
462 to parr growth and body size (Økland *et al.*, 1993) and an increase in temperature will
463 increase growth rate (Forseth *et al., 2*001) provided that there is no limitation to food supply.
464 Water temperatures in summer were higher in all future scenarios than in control scenarios.
465 This resulted in increased parr growth rates and reduced age at smolt migration (typically at
466 age 2+ rather than age 3+ in the control scenario). Smoltification at a younger age meant that
467 parr individuals were experiencing a shorter total period of parr density dependent mortality
468 (between parr recruitment and smoltification). For the ECHAM.Reg.B2 scenario this caused a
469 net increase in smolt abundance. For the other three scenarios, the magnitude of increased

This is the accepted version of an article published in Science of the Total Environment
DOI: 10.1016/j.scitotenv.2018.03.058

density dependent mortality caused by the large reduction in wetted area cancelled out the effect of the shorter period of density dependent mortality associated with earlier smoltification, and caused reduced smolt abundance compared to the control scenarios. Thus, this study shows that an increase in temperature in future climates in the study area has a positive effect on the abundance of smolt, by shortening the time from hatching to smoltification, that may or may not be cancelled by other negative effects of climate change. A similar result, such as faster growth of parr (Beer & Anderson 2013) and younger smolt ages due to fast growth, has also been shown by Hedger *et al*. (2013b) and Leppi *et al*. (2014). Further, simulating future climate change in the southern distribution range of Atlantic salmon, Piou & Prevost (2013) showed an increase in parr growth and population size, with increased future river temperatures, but no change in smolt age. However, in the population they studied Atlantic salmon smoltified as 1-year olds and a decrease in smolt age was thus not possible. Nevertheless, in populations where Atlantic salmon smoltify from 2-years and older, a relatively small increase in water temperature could have a potentially large influence on smolt abundance. If a large proportion of parr is just below the size required for smoltification in spring, a small increase in temperature could potentially have a large effect on the annual turnover of smolts by enabling these to smoltify at a younger age.

This study contributes to the understanding of mechanisms influencing freshwater Atlantic salmon populations under conditions of a climate-induced change in discharge and water temperature. However, it is important to stress that the model presents a simplified conceptualization of an Atlantic salmon population and does not contain all factors that may influence the population. The results should be viewed as one possible outcome of climate change, but with the notion that there are alternative possible outcomes if additional factors are added or changed. The modelling in the current study focused on the freshwater phase,

This is the accepted version of an article published in Science of the Total Environment
DOI: 10.1016/j.scitotenv.2018.03.058

and potential future climate changes in the marine phase were not studied. However, it is likely that climate change also will affect the marine phase of the life cycle of Atlantic salmon, particularly traits such as post-smolt growth, sea survival and the timing of spawning migration (Jonsson & Jonsson, 2009) which may affect the subsequent population abundance in the freshwater phase through determining the number and size distribution of returning spawners.

4.2 Mitigation of effect of climate change on freshwater salmon abundance

In the three future scenarios that predicted the lowest wetted area (Had.Reg.A2, Had.Reg.B2 and ECHAM.Nor.B2), there was a strong positive influence on parr and smolt abundance from implementing minimum discharge regimes. Parr and smolt abundance increased correspondingly with an increase in minimum discharge from 2 m^3s^{-1} up to 10 m^3s^{-1}. Thus, increasing the minimum discharge during summer months had a positive long-term effect on the abundance of Atlantic salmon smolt.

An unknown indirect effect of climate change in regulated rivers is the future demand for energy. The hydropower production model nMAG was run in this study with the present regulation pattern, which is a result of today's energy market and consumption pattern of energy. However, this regulation pattern will probably change in the future to adapt to the future climate conditions and energy demands. Such an adaptation may be to change the time and pattern for when reservoirs are emptied, to reduce flood loss and spilling in winter. If more winter water is stored in the future, it may be possible to use this water in summer, i.e. as a mitigation measure to counteract the negative effects of very low discharges (and correspondingly wetted area) in the abundance of Atlantic salmon smolts.

A general trend in future scenarios for Southern Norway is increased winter precipitation and reduced summer precipitation (Schneider *et al.*, 2013). The fact that the Mandalselva is

This is the accepted version of an article published in Science of the Total Environment
DOI: 10.1016/j.scitotenv.2018.03.058

518 regulated and has reservoir capacity to store water, may benefit the Atlantic salmon
519 population in a future climate because it allows for the possibility of releasing water from
520 reservoirs for the Atlantic salmon population in critical periods (see Piou & Prevost, 2013).
521 To use minimum discharge as a mitigation measure requires reservoirs with storage capacity.
522 Atlantic salmon is found in rivers that flow into the North Atlantic, in Europe and North
523 America. Within these continents, there are 3518 reservoirs listed in the FAO AQUASTAT
524 database (fao.org/NR/WATER/aquastat/main/index.stm), where 42 % have a storage capacity
525 above 100 million m^3 and 21 % have a storage capacity of at least 300 million m^3. These
526 numbers suggest that there is considerable storage capacity, although it is unknown how many
527 of these reservoirs are connected to rivers with Atlantic salmon populations and further how
528 many of these populations are in need of future mitigation measures. However, to compare
529 different river systems and mitigation measures, detailed knowledge of hydrology,
530 hydropower systems, channel hydraulics, and the local fish populations needs to be combined.
531 As an example, bottlenecks for other Atlantic salmon populations may not be the same as for
532 the population in the Mandalselva, depending on climate projections, the power system and
533 other local factors. For instance, future climate change projections for Western Norway
534 predict higher discharges from summer to winter (Hedger et al. 2013b) and in such systems a
535 low wetted area in summer may not be the bottleneck. In unregulated rivers and in regulated
536 rivers with a low reservoir capacity, it may be possible to implement other mitigation
537 measures, such as restoration of habitat, but such methods may not be as effective as direct
538 mitigation of hydrological impacts (in addition to other mitigation measures) (Battin *et al.*,
539 2007). However, this depends on the specific bottleneck for each fish population.

This is the accepted version of an article published in Science of the Total Environment
DOI: 10.1016/j.scitotenv.2018.03.058

5. CONCLUSION

This study simulates how future climate change may result in reduced Atlantic salmon abundance in rivers where discharge during summer is reduced. Reduced discharge may result in reductions in wetted area, and consequent reductions in river carrying capacity. Lower carrying capacities lead to reduced juvenile abundance. However, by simulating different regulated minimum discharge regimes, this study also shows that regulated rivers with reservoir capacity may contribute to future mitigation solutions for Atlantic salmon populations by allowing for release of water from reservoirs during critical periods for juvenile Atlantic salmon. These results are specific to the regional climate examined – reduced summertime precipitation is not predicted for all parts of the world. However, this simulation approach can be applied to regulated rivers in different regions to identify potential bottlenecks in Atlantic salmon survival, enabling remediation strategies to be devised.

6. ACKNOWLEDGEMENTS

We would like to thank the anonymous reviewers for providing valuable comments on manuscripts drafts. Funding was provided by the Norwegian Research Council (NFR) via the Environmentally Designed Operation of Regulated Rivers project (EnviDORRclimate).

This is the accepted version of an article published in Science of the Total Environment
DOI: 10.1016/j.scitotenv.2018.03.058

7. REFERENCES

Alfredsen K, Harby A, Linnansaari T, Ugedal O (2012) Development of an inflow-controlled environmental flow regime for a Norwegian river. River Research and Applications, **28**, 731-739.

Angilletta MJ, Niewiarowski PH, Navas CA (2002) The evolution of thermal physiology in ectotherms. Journal of Thermal Biology, **27**, 249-268.

Battin J, Wiley MW, Ruckelshaus MH, Palmer RN, Korb E, Bartz KK, Imaki H (2007) Projected impacts of climate change on salmon habitat restoration. Proceedings of the National Academy of Sciences of the United States of America, **104**, 6720-6725.

Beer WN, Anderson JJ (2013) Sensitivity of salmonid freshwater life history in western US streams to future climate conditions. Global Change Biology, **19**, 2547-2556.

Christensen OB, Drews M, Christensen JH, Dethloff K, Ketelsen K, Hebestadt I, Rinke A, (2007) The HIRHAM Regional Climate Model Version 5 (beta). Danish Meteorological Institute, www.dmi.dk/dmi/tr06-17.

DeAngelis DL, Grimm V (2014) Individual-based models in ecology after four decades. F1000Prime Rep, **6**, 39 pp.

Einum S, Sundt-Hansen L, Nislow KH (2006) The partitioning of density-dependent dispersal, growth and survival throughout ontogeny in a highly fecund organism. OIKOS, **113**, 489-496.

Einum S, Fleming IA (2007) Of chickens and eggs: Diverging propagule size of iteroparous and semelparous organisms. Evolution, **61**, 232-238.

This is the accepted version of an article published in Science of the Total Environment
DOI: 10.1016/j.scitotenv.2018.03.058

578 Engen-Skaugen T (2007) Refinement of dynamically downscaled precipitation and
579 temperature scenarios. Climate Change **84**, 365–382.

580 Engen-Skaugen T, Haugen JE & Hanssen-Bauer I (2008). Dynamically downscaled climate
581 scenarios available at the Norwegian Meteorological Institute – per December 2008,
582 met.no report no. 24/2008.

583 Fjeldstad HP, Alfredsen K, Boissy T (2014) Optimising Atlantic salmon smolt survival by use
584 of hydropower simulation modelling in a regulated river. Fisheries Management and
585 Ecology, **21**, 22-31.

586 Forseth T, Hurley MA, Jensen AJ, Elliott JM (2001) Functional models for growth and food
587 consumption of Atlantic salmon parr, *Salmo salar*, from a Norwegian river. Freshwater
588 Biology, **46**, 173-186.

589 Gibson RJ, Myers RA (1988) Influence of seasonal river discharge on survival of juvenile
590 Atlantic salmon, *Salmo salar*. Canadian Journal of Fisheries and Aquatic Sciences, **45**,
591 344-348.

592 Hanssen-Bauer I, Førland EJ, Haddeland I *et al.* (Red.) (2015) Klima i Norge 2100 -
593 Kunnskapsgrunnlag for klimatilpasning oppdatert i 2015, Norsk Klimaservicesenter
594 rapport 2/2015 (NCCS report no. 2/2015), Oslo. (In Norwegian.)

595 HEC-RAS 2008. User manual. US Army Corps of Engineers, Hydrologic Engineering Center,
596 Davis Version 4.0, 2008.

597 Hedger RD, Sundt-Hansen LE, Forseth T, Diserud OH, Ugedal O, Finstad AG (2013a)
598 Modelling the complete life-cycle of Atlantic salmon (*Salmo salar L.*) using a spatially
599 explicit individual-based approach. Ecological Modelling, **248**, 119-129.

This is the accepted version of an article published in Science of the Total Environment
DOI: 10.1016/j.scitotenv.2018.03.058

600 Hedger RD, Sundt-Hansen LE, Forseth T, Ugedal O, Diserud OH, Kvambekk AS, Finstad
601 AG (2013b) Predicting climate change effects on subarctic-Arctic populations of
602 Atlantic salmon (*Salmo salar*). Canadian Journal of Fisheries and Aquatic Sciences, **70**,
603 159-168.

604 Heino J, Virkkala R, Toivonen H (2009) Climate change and freshwater biodiversity: detected
605 patterns, future trends and adaptations in northern regions. Biological Reviews, **84**, 39-
606 54.

607 Hesthagen T. (ed.). 2010. Reetablering av laks på Sørlandet. Etablering av nye laksestammer i
608 Mandalselva og Tovdalselva etter kalking. DN-utredning. (In Norwegian.)

609 Hindar K, Hutchings JA, Diserud O, Fiske P (2011) Stock recruitment and exploitation. In:
610 *Atlantic Salmon Ecology* (eds. Aas Ø, Einum S, Klemetsen A, Skurdal J), pp. 299–332.
611 Blackwell Publishing Ltd., Oxford, UK.

612 Hvidsten NA, Diserud OH, Jensen AJ, Jensas JG, Johnsen BO, Ugedal O (2015) Water
613 discharge affects Atlantic salmon *Salmo salar* smolt production: a 27 year study in the
614 River Orkla, Norway. Journal of Fish Biology, **86**, 92-104.

615 ICES (2013) Report of the Working Group on North Atlantic Salmon (WGNAS), 26 March–4
616 April 2012, Copenhagen, Denmark. ICES CM 2012/ACOM:09. 323 pp.

617 IPCC (2007) In: Climate Change 2007. The Physical Science Basis. Contribution of Working
618 Group I to the Fourth Assessment Report of the IPCC (Eds. Solomon S, Qin S,
619 Manning M, Chen Z, Marquis M, Averyt KB, Tignor M, Miller H.L.) PP 996.
620 University Press, Cambridge.

This is the accepted version of an article published in Science of the Total Environment
DOI: 10.1016/j.scitotenv.2018.03.058

621 IPCC (2014) Climate Change 2014: Synthesis Report. Contribution of Working Groups I, II
622 and III to the Fifth Assessment Report of the Intergovernmental Panel on Climate
623 Change [Core Writing Team, R.K. Pachauri and L.A. Meyer (eds.)]. IPCC, Geneva,
624 Switzerland, 151 pp.

625 Jonsson B, Forseth T, Jensen AJ, Naesje TF (2001) Thermal performance of juvenile Atlantic
626 Salmon, *Salmo salar* L. Functional Ecology, **15**, 701-711.

627 Jonsson B, Jonsson N (2009) A review of the likely effects of climate change on anadromous
628 Atlantic salmon *Salmo salar* and brown trout *Salmo trutta*, with particular reference to
629 water temperature and flow. Journal of Fish Biology, **75**, 2381-2447.

630 Killingtveit Å, Sælthun NR (1995) Hydrology. Volume 7 in the Hydropower Development
631 series. Trondheim: Norwegian Institute of Technology, 213 pp.

632 Killingtveit Å (2004) nMAG User Manual; Norwegian Institute of Technology, Division of
633 Hydraulic Engineering: Trondheim, Norway.

634 Kolberg S, Bruland O (2012) ENKI – An open source environmental modelling platform.

635 Kolberg S, Rue H, Gottschalk L (2006) A Bayesian spatial assimilation scheme for snow
636 coverage observations in a gridded snow model. Hydrology and Earth System Sciences,
637 **10**, 369-381.

638 Knouft JH. DL Ficklin (2017) The potential impacts of climate change on biodiversity in
639 flowing freshwater systems. In Futuyma, D. J. (ed) Annual Review of Ecology,
640 Evolution, and Systematics, Annual Review of Ecology Evolution and Systematics,
641 Annual Reviews, Palo Alto, **48**, 111-133.

This is the accepted version of an article published in Science of the Total Environment
DOI: 10.1016/j.scitotenv.2018.03.058

642 Leppi JC, Rinella DJ, Wilson RR, Loya WM (2014) Linking climate change projections for
643 an Alaskan watershed to future coho salmon production. Global Change Biology, **20**,
644 1808-1820.

645 May W (2007) The simulation of the variability and extremes of daily precipitation over
646 Europe by the HIRHAM regional climate model. Global and Planetary Change, **57**, 59-
647 82.

648 Metcalfe NB, Fraser NHC, Burns MD (1998) State-dependent shifts between nocturnal and
649 diurnal activity in salmon. Proceedings of the Royal Society of London Series B-
650 Biological Sciences, **265**, 1503-1507.

651 Nash JE, Sutcliffe JV (1970). River flow forecasting through. Part I. A conceptual models
652 discussion of principles. Journal of Hydrology, **10**, 282–290.

653 Piou C, Prevost E (2013) Contrasting effects of climate change in continental vs. oceanic
654 environments on population persistence and microevolution of Atlantic salmon. Global
655 Change Biology, **19**, 711-723.

656 Ratkowsky D, Lowry R, Mcmeekin T, Stokes A, Chandler R (1983) Model for bacterial
657 culture growth rate throughout the entire biokinetic temperature range. Journal of
658 Bacteriology, **154**, 1222-1226.

659 Rinde T (2000) LandPine: En hydrologisk modell for simulering av arealbruksendringers
660 innvirkning på avrenningsforhold. Hydra rapport nr. N04, Norges vassdrags- og
661 energidirektorat, Oslo. ISBN 82-410-0390-0 h (In norwegian).

This is the accepted version of an article published in Science of the Total Environment
DOI: 10.1016/j.scitotenv.2018.03.058

662 Sauterleute JF, Hedger RD, Hauer C, Pulg U, Skoglund H, Sundt-Hansen LE, Bakken TH,
663 Ugedal, O (2016) Modelling the effects of stranding on the Atlantic salmon population
664 in the Dale River, Norway. Science of the Total Environment, **573**, 574-584.

665 Schneider C, Laize CLR, Acreman MC, Florke M (2013) How will climate change modify
666 river flow regimes in Europe? Hydrology and Earth System Sciences, **17**, 325-339.

667 Ugedal O, Larsen BM, Forseth T, Johnsen BO (2006). The production capacity for Atlantic
668 salmon and estimated losses due to hydropower regulation in the River Mandalselva.
669 NINA Report 146, p 46. (In Norwegian).

670 Ugedal O, Naesje TF, Thorstad EB, Forseth T, Saksgard LM, Heggberget TG (2008) Twenty
671 years of hydropower regulation in the River Alta: long-term changes in abundance of
672 juvenile and adult Atlantic salmon. Hydrobiologia, **609**, 9-23.

673 Van Vuuren DP, Carter TR (2014) Climate and socio-economic scenarios for climate change
674 research and assessment: reconciling the new with the old. Climatic Change, **122**, 415-
675 429.

676 Williams NE, O'Brien ML, Yao X (2017) Using Survey Data for Agent-Based Modeling:
677 Design and Challenges in a Model of Armed Conflict and Population Change. In:
678 *Agent-Based Modelling in Population Studies: Concepts, Methods, and Applications.*
679 (eds Grow A, Van Bavel J) pp. 159-184 Page. Cham, Springer International Publishing.

680 Windsor ML, Hutchinson P, Hansen LP, Reddin DG (2012) Atlantic salmon at sea: findings
681 from recent research and their implications for management. NASCO document
682 CNL(12)60. Edinburgh, UK: 20 pp. [www document]. URL
683 http://www.nasco.int/pdf/reports_other/Salmon_at_sea.pdf

This is the accepted version of an article published in Science of the Total Environment
DOI: 10.1016/j.scitotenv.2018.03.058

684 Økland F, Jonsson B, Jensen AJ, Hansen LP (1993) Is there a threshold size regulating
685 seaward migration of brown trout and Atlantic salmon? Journal of Fish Biology, **42**,
686 541-550.

This is the accepted version of an article published in Science of the Total Environment
DOI: 10.1016/j.scitotenv.2018.03.058